Joint Position and Clock Tracking of Wireless Nodes Under Mixed LOS-NLOS Conditions

Juan Pablo Grisales Campeón[a,b], Pablo I. Fierens[a,b]

[a] *Instituto Tecnológico de Buenos Aires (ITBA), Ciudad de Buenos Aires, C1106ACD Argentina*
[b] *Consejo Nacional de Investigaciones Científicas y Técnicas (CONICET), Ciudad de Buenos Aires, C1425FQB Argentina*

Abstract

We propose an algorithm for the simultaneous position and clock tracking of a wireless mobile node by a set of reference nodes. Based on a protocol similar to that of two-way ranging, our algorithm efficiently estimates the position and velocity of the mobile, and the skew and offset of its clock. We take into account that the propagation conditions between each reference node and the mobile change as the latter moves. In particular, changes between line-of-sight (LOS) and several non-line-of-sight (NLOS) scenarios are considered. We study the performance of our algorithm and compare it to other relevant proposals in the literature by means of simulations, showing that our proposed method improves localization accuracy.

Keywords: Positioning, synchronization, NLOS.

1. Introduction

Due to the relevance of location-based services and applications, the tracking of wireless devices has been the focus of intense research during the last two decades. Most localization approaches are based on measurements of the received signal strength (RSS), angle of arrival (AOA), time of arrival (TOA), or time difference of arrival (TDOA) (see Refs. [1–6] and references therein).

In this work, we focus on TOA measurements. Intuitively, for positioning with TOA techniques, what really matters are the distances between a mobile node whose location is required and a number of reference or anchor nodes. Under line-of-sight (LOS) conditions, those distances are proportional to the time it takes a signal to travel between the mobile and the anchors. Each time of flight can be estimated from a TOA measurement at each anchor if the exact sending time is known. This requires the clocks of the mobile node and the anchors to be synchronized. Let us focus on this problem as it is most relevant for understanding the motivation of this paper. The distance between a mobile node and an anchor can be estimated as

$$d = c \times (t_a - t_s)\,, \tag{1}$$

where t_a is the time-of-arrival of a wireless signal to the anchor, t_s is the time when the signal was sent from the mobile node, and c is the speed of light. In this equation we have arbitrarily assumed that the communication was initiated by the mobile node. The sending time can be communicated by the mobile in a message. If the mobile and the reference nodes are not perfectly synchronized, there may be an error in the time measured, say, at the mobile. For example, the sending time measured and communicated by the mobile to the anchor can be written as $\tau_s = t_s + \phi$, where ϕ is an offset due to lack of synchronization. Under this setting, the estimated distance would be

$$\hat{d} = c \times (t_a - \tau_s) = c \times (t_a - t_s - \phi) = d - c \times \phi. \tag{2}$$

As an example, a value of $\phi = 0.5$ µs corresponds to an error of ~ 15 cm. A common solution is to use two-way ranging [1]. In this scheme a message is sent from, say, the mobile to the anchor and it is immediately replied so both the sending and final arrival times are measured at the mobile. If the measured sending and arrival times can be written as $\tau_s = t_s + \phi$ and $\tau_a = t_a + \phi$, where t_s and the t_a are the actual times, then the distance can be estimated as

$$\hat{d} = c \times \frac{(\tau_a - \tau_s)}{2} = c \times \frac{(t_a + \phi - t_s - \phi)}{2} = c \times \frac{(t_a - t_s)}{2} = d, \tag{3}$$

where the factor of two is due to the two-way nature of the communication. This procedure appears to solve the problem, but only because we have considered the lack of synchronization as modeled by a constant offset. Time measurements are based on a local oscillator whose frequency may not be perfectly constant and drifts slowly from its nominal value, specially in cheaper nodes [7–9]. Thus, in general, measured times are better modeled by $\tau_s = \omega \times t_s + \phi$ and $\tau_a = \omega \times t_a + \phi$, where ω represents the clock drift and it is close to unity. In this case, the estimated distance reads

$$\hat{d} = c \times \frac{(\tau_a - \tau_s)}{2} = \omega \times c \times \frac{(t_a + \phi - t_s - \phi)}{2} = \omega \times d. \tag{4}$$

As an example, if $|\omega - 1| = 2 \times 10^{-5}$ and $d = 500$ meter, the estimation error would be of the order of 1 cm. We must also observe that the drift ω and the offset ϕ of the local clock are not constant in general and their changes must be tracked (see, e.g., [10, 11] and references therein).

In several practical situations, we may expect to have better local oscillators in the reference nodes, as they may correspond to higher cost fixed communication infrastructure (e.g., base transceiver stations in a cellular network or access points in a WiFi network). In these cases, it is reasonable to assume that the influence of the anchor's clock inaccuracies are negligible. Indeed, this is one of the assumptions of this work. Under this setting, it is worth it to reverse the order of the communication so it is the anchor that initiates the two-way exchange. If the drift of the local oscillator at the reference node is $\omega = 1$ (a perfect clock), then the estimation in Eq. (4) would be perfect. However, Eq. (4) assumes that the reply is *immediate*. This is an unreasonable assumption as there is always a necessary processing time, say t_p. Thus, when the anchor node initiates the exchange, the estimated distance can be written as

$$\hat{d} = c \times \frac{(\tau_a - \tau_s)}{2} = c \times \frac{(t_a + \phi - t_s - \phi)}{2} = d + c \times \frac{t_p}{2}. \tag{5}$$

The reply processing time may be modeled, in general, as a random variable.

If the mobile node measures t_p, it would include the errors due to its clock inaccuracies and, thus, we would be back to the same problems we have when the two-way exchange is initiated by mobile node. There are several ways out of this conundrum. For example, we can resort to TDOA, requiring only the perfect synchronization of the reference nodes [1], or we can thrive to keep the clock of the mobile node as perfectly synchronized as possible (see, e.g., [12–16] and references therein for more information on network synchronization). In Ref. [17] we proposed a different approach by simultaneously tracking the position and the clock of the mobile based on TOA measurements at the mobile and anchor nodes. The core of our proposal was the assumption that, though random, t_p can be, in general, upper bounded. This upper bound allowed us to impose a fixed deterministic reply time δ ($> t_p$). The fact that δ was inaccurately measured at the mobile node enabled the estimation of its clock drift ω. More details on our solution can be found in Ref. [17], but let us mention that the explicit estimation of the distances between the mobile node and the anchors is avoided, proceeding to estimate directly the position and the velocity of the mobile and the drift and the offset of its clock.

We must note that there are other works in the literature on the simultaneous positioning and synchronization problem [18–21]. However, to the best of our knowledge, only line-of-sight (LOS) scenarios were considered in most cases. In the presence of a non-line-of-sight (NLOS) channel, an extra delay Γ must be added to the time of flight of wireless signals. In this case, the simplest range estimation in Eq. (3) becomes

$$\hat{d} = c \times \frac{(\tau_a - \tau_s)}{2} = c \times \frac{(t_a - t_s)}{2} + c \times \Gamma = d + c \times \Gamma, \tag{6}$$

where we have assumed that the NLOS delay is the same in both directions, and Γ is usually modeled as a random variable. There is a vast literature on the mitigation of NLOS positioning errors (see, e.g., [21–69] and references therein). Although a complete review of the area is beyond of the scope of this paper, for our purposes we can divide the literature in three main approaches. First, there are many proposals that assume no further information than the time-of-arrival or time-difference-of-arrival measurements. In these cases, either no (except for its positivity) or little knowledge (such its probability distribution) is assumed about Γ. Second, there is a group of papers that assume that certain characteristics of the received signal may indicate the presence of a NLOS condition. For example, the kurtosis of the estimated channel impulse response or the root mean square (RMS) delay spread have been proposed as statistics for the detection of NLOS channels in the presence of multipath fading. Finally, there is a third approach which consists on the fusion of TOA observations with other measurements, such as AOA. The development in this work falls mainly in the second group. However, since we want the core of our proposal to be applicable to a wide variety of communication networks, we avoid any details of the actual physical channel, like its multipath fading characteristics. Following the work of Huerta et al. [51], we assume that any channel-related measurement can be summarized in a test statistic that gives an indication of the NLOS condition. This abstraction has the advantage of generality and paves the way for the specialization of our proposal to any given physical layer of communication and receiver structure. Furthermore, it enables us to extend the Improved Unscented Kalman Filter (IUKF) developed in Ref. [51] to the context of our problem, as explained in Section 4.

A special comment is due about the work of Wu et al. [21] as, to the best of our knowledge, is the only paper in the literature that deals with the simultaneous positioning and synchronization problem under NLOS conditions on the basis of TOA measurements. The proposal in Ref. [21], however, has two limitations: only a stationary mobile node is considered, and the synchronization error is modeled by a constant offset. In this paper we lift both limitations as we consider a moving node and a more complex model of the inaccuracies of its local oscillator.

Interestingly, most of the literature focuses on only two possible channel conditions, either LOS or NLOS. However, it has been noted that this is only a rough approximation to more complex situations where different types of non-line-of-sight conditions can be distinguished. For example, Pahlavan et al. [36] (see also Refs. [44, 45, 70]) described two different channel profiles associated with NLOS conditions in UWB-based TOA measurements. It is worth it to describe the reasoning behind these different types of NLOS conditions. Let us consider the channel impulse response modeled as

$$h(t) = \sum_{k=1}^{L} g_k \delta(t - s_k), \tag{7}$$

where L is the number of multipath components, and $g_k \in \mathbb{C}$ and $s_k \in \mathbb{R}^{\geq 0}$ correspond to the amplitude and TOA of the kth path, respectively. As it is customary, let us assume that $s_{k+1} > s_k$. The receiver estimates the time of arrival of the signal as that of the *first detected path*. The key here is the word *detected*. Indeed, in the usual LOS condition and for not too long distances, the first detected path will correspond to that of the direct path and TOA $= s_1$. Nonetheless, there may be an estimation error due to the multipath condition and other noise sources. Whenever the power of the first path ($\propto |g_1|^2$) falls below a receiver-specific threshold, the direct path can be considered as *undetected*. This situation is analog to the usual NLOS condition in the literature, and the time of arrival is estimated on the basis of a secondary path, that is, from s_k for some $k > 1$. Moreover, the authors of Ref. [36] distinguish two different cases. In the first case, the direct path is undetected (e.g., because it is blocked by a large metallic object), but the total signal power ($\propto \sum |g_k|^2$) is high (probably because the distance is small). In the second case, not only the direct path is blocked, but the total power is small (probably because the transmitter and the receiver are far apart). In the latter case, the authors observe larger TOA estimation errors than in the former; these are the two types of NLOS conditions.

Other authors have used more than one type of NLOS condition [38, 62, 67, 71, 72]. In particular, in the area of UWB channels, it is common to use the terms *soft* and *hard* to distinguish between two different NLOS conditions [38, 71]. Thus, we shall also refer to LOS, soft NLOS and hard NLOS conditions in some numerical experiments in this paper. Nonetheless, we consider that, in general, more than two non-line-of-sight conditions are possible. Indeed, in very complex physical channels, very different "typical" multipath fading profiles or channel impulse responses are possible. For this reason, we shall also speak of *sight conditions*, referring to any of those characteristic channels. We must note that, to the best of our knowledge, the problem of joint positioning and synchronization of a wireless node under several sight conditions has not been studied.

In the case of a fixed indoor plan, changes in the channel between the mobile node and each reference anchor can be modeled on the basis of the route followed by the mobile. Although this detailed physical modeling approach is possible, it is also specific to a given indoor plan. For this reason, most of the literature models changes between different sight conditions by means of Markov chains [33, 34, 44, 45, 50, 51, 56]. Furthermore, it is reasonable to model the corresponding transition probabilities as dependent on the velocity of the mobile node, as it is done in Refs. [34, 45, 51]. In particular, Huerta and colleagues [34, 51] use their proposed relation between the transition probabilities and the mobile velocity to estimate the former from the estimation of the latter. Since these velocity-dependent models are peculiar to the physical characteristics of the wireless network and the type of indoor environment under consideration, and for the sake of generality, we use essentially fixed transition probabilities in our modeling approach.

In summary, in this paper we study the problem of simultaneously tracking a mobile node and the characteristics of its local oscillator based on TOA measurements on the same node and a set of reference (anchor) nodes, under varying LOS/NLOS conditions. This work's contributions can be outlined as follows:

- We propose an algorithm to track the position, velocity and parameters of the clock of a mobile wireless node by a set of reference nodes.

- The algorithm accounts for the fact that the propagation channel between the mobile node and each anchor may change from LOS to several different types of NLOS.

The remaining of the paper is organized as follows. Section 2 summarizes the system model and Section 3 explains the details of the observation protocol. Section 4 describes the proposed solution. Performance of our proposal is evaluated and compared to that of other algorithms in Section 5. Finally, we close with some final remarks in Section 6.

2. System Model

In this section we present some details beyond the generalities anticipated in the Introduction. Even though time is considered a continuous variable, most of the modeling approach is based on time discretized in epochs of length h. That is, we assume that changes in the system model occur at times $t_k = k \times h$ with $k \in \mathbb{N}^0$.

2.1. Clock Inaccuracies

The local oscillator at the wireless mobile node can be characterized by its offset ϕ and drift (or skew) ω [73, 74]. In particular, time measured at the mobile node can be written as

$$\tau = \omega \times t + \phi + n, \tag{8}$$

where t is the actual time and n is a measurement noise which we assume zero-mean Gaussian, i.e., $n \sim \mathcal{N}(0, \sigma_m^2)$. Usual values for ω, ϕ and time measurement noise can be found in Refs. [9, 75].

We model variations of clock parameters due, e.g., to temperature changes and other factors, by means of Gaussian random walks. Although this is a simplification of more complex clock models in the literature [10, 11, 76, 77], it is sufficient for our purposes here. In particular, we let

$$\omega_k = \omega_{k-1} + u^{\omega}_{k-1}, \qquad \phi_k = \phi_{k-1} + u^{\phi}_{k-1}, \tag{9}$$

where $u^{\omega}_{k-1} \sim \mathcal{N}(0, \sigma^2_\omega)$ and $u^{\phi}_{k-1} \sim \mathcal{N}(0, \sigma^2_\phi)$ are independent.

We assume that anchors have local oscillators with negligible inaccuracies and which are perfectly synchronized. Nonetheless, even anchor nodes may incur in errors when measuring times of arrival. As it was already explained, these errors may be partially due to multipath fading, even in the presence of a LOS condition. For the sake of simplicity, we also model the measurement noise at the reference nodes as $\mathcal{N}(0, \sigma^2_m)$.

We must note that only the standard deviations σ_ω, σ_ϕ and σ_m are assumed to be known, while all other parameters must be estimated.

2.2. Mobility Model

We use the Gauss-Markov Mobility Model [78] for the mobile node. In particular, we assume that its velocity behaves as a random walk with uncorrelated Gaussian steps. Let $\vec{v}_k = (v^x_k, v^y_k)^T$ denote the mobile velocity at time t_k, $\vec{x}(t)$ the position at time t and $\vec{x}_k = (x_k, y_k)^T = \vec{x}(t_k)$. Then, we describe the motion of the node by

$$\vec{v}_k = \vec{v}_{k-1} + \begin{pmatrix} u^{v_x}_{k-1} \\ u^{v_y}_{k-1} \end{pmatrix}, \tag{10}$$

$$\vec{x}(t) = \vec{x}_k + \vec{v}_k \times (t - t_k) \qquad \text{for } t \in [t_k, t_{k+1}], \tag{11}$$

where $u^{v_x}_{k-1}, u^{v_y}_{k-1} \sim \mathcal{N}(0, \sigma^2_v)$ are independent. We must remark that the mobility model is not essential for our proposed solution to the problem of mobile and clock tracking. Indeed, what is relevant is that there is a *known* model. However, the simplicity of the previous equations facilitate numerical experiments.

For the sake of simplicity, anchor nodes are assumed to be stationary. Nonetheless, it is straightforward to extend our results to moving anchors with perfectly known positions.

2.3. Sight Condition

As it was explained in Section 1, we consider several sight conditions, either LOS or different types of NLOS channels. Let us call N_z the number of such conditions. We shall refer to each sight situation by $z \in \{0, 1, \cdots, N_z - 1\}$, where we reserve the value $z = 0$ for the LOS channel. Time-of-arrival measurements are offset by a random variable Γ with distribution $F_z(t)$.

We model changes in the sight situation by means of a Markov chain with transition matrix $\mathbf{Q} \in \mathbb{R}^{N_z \times N_z}$ such that $\mathbf{Q}_{i,j} = P(z = j | z = i)$ is the transition probability from sight condition i to sight condition j. Transitions occur at multiples K_{sight} of the time epoch h.

The number of relevant sight situations N_z, the distributions F_z, the transition matrix $\mathbf{Q}$ and K_{sight} can be estimated by a prior onsite survey, as it is done in Refs. [44, 45]. Although it is desirable to avoid this offline step and to allow for the online estimation of these parameters, we shall assume them known in this work.

2.4. Summary of the System Model

At each time t_k, the system is characterized by two vectors

$$\vec{s}_k = \left(\omega_k,\, \phi_k,\, v_k^x,\, v_k^y,\, x_k,\, y_k\right)^T, \tag{12}$$

$$\vec{z}_k = \left(z_k^0,\, z_k^1,\, \cdots,\, z_k^{N_a - 1}\right)^T, \tag{13}$$

where z_k^i is the sight situation between the mobile node and the ith reference node and N_a is the number of anchors. Although the complete system state can be modeled as a single vector resulting from the concatenation of $\vec{s}_k$ and $\vec{z}_k$, this particular separation facilitates the explanation of our proposed algorithm. The evolution of $\vec{s}_k$ can be written as (cf. Eqs. (9)-(11))

$$\vec{s}_k = \mathbf{F}\, \vec{s}_{k-1} + \mathbf{G}\, \vec{u}_{k-1}, \tag{14}$$

where $\vec{u}_{k-1} \sim \mathcal{N}(\vec{0}, \mathbf{R}^u)$ with $\mathbf{R}^u = \mathrm{diag}(\sigma_\omega^2, \sigma_\phi^2, \sigma_v^2, \sigma_v^2)$, and

$$\mathbf{F} = \begin{pmatrix} 1 & 0 & 0 & 0 & 0 & 0 \\ 0 & 1 & 0 & 0 & 0 & 0 \\ 0 & 0 & 1 & 0 & 0 & 0 \\ 0 & 0 & 0 & 1 & 0 & 0 \\ 0 & 0 & h & 0 & 1 & 0 \\ 0 & 0 & 0 & h & 0 & 1 \end{pmatrix}, \qquad \mathbf{G} = \begin{pmatrix} 1 & 0 & 0 & 0 \\ 0 & 1 & 0 & 0 \\ 0 & 0 & 1 & 0 \\ 0 & 0 & 0 & 1 \\ 0 & 0 & 0 & 0 \\ 0 & 0 & 0 & 0 \end{pmatrix}. \tag{15}$$

Changes in the sight condition are modeled as a Markov chain with stochastic matrix $\mathbf{Q}$, where changes can occur only at multiples K_{sight} of the observation period. Since time is discretized at a finer granularity, it is convenient to described the evolution of $\vec{z}_k$ as modeled by the non-homogeneous Markov chain

$$P\left(z_k^i = j \,\middle|\, z_{k-1}^i = m\right) = \begin{cases} \mathbf{I}_{mj} & \text{if } k \neq rK_{\text{sight}}, \\ \mathbf{Q}_{mj} & \text{if } k = rK_{\text{sight}}, \end{cases} \tag{16}$$

for $r \in \mathbb{N}$, $i = 0, 1, \cdots, N_a - 1$, and where $\mathbf{I}$ is the $N_z \times N_z$ identity matrix.

3. Measurement Protocol and Observation Model

The observation model consists of two main parts, the TOA measurement protocol, described in Section 3.1, and the test statistics related to the sight situations as explained in Section 3.2.

3.1. Measurement Protocol

Our system is based on the measurement protocol which we proposed in Ref. [17] and is shown in Fig. 1. For the sake of completeness, we summarize this protocol as follows:

1. The kth observation round starts at time $t_k = kh$, where h is a fixed time period.

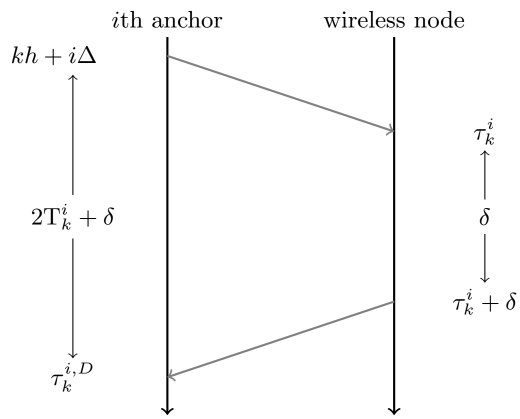

Figure 1: Measurement protocol. Time is discretized into observation periods of length h. A time $i\Delta$ after the beginning of the kth observation period, the ith anchor exchanges two messages with the wireless node. Time measurement noise and the effect of clock skew and offset are not shown for clarity.

2. The ith reference node ($i = 0, 1, \cdots, N_a - 1$) is expected to send a message to the mobile at time $t_k + i\Delta$, where Δ is such that $N_a\Delta < h$. Due to measurement noise at the anchor, the actual sending time is $t_k + i\Delta + n_k^{i,A}$, where $n_k^{i,A} \sim \mathcal{N}(0, \sigma_m^2)$.
3. The mobile node records the arrival of the message at time

$$\tau_k^i = \omega_k \times \left(t_k + i\Delta + n_k^{i,A} + \frac{d_k^i}{c} + \Gamma_k^i \right) + \phi_k + n_k^{i,B}, \qquad (17)$$

where ω_k and ϕ_k are the mobile clock skew and offset, respectively, d_k^i is the traveled distance, c is the speed of light, and $n_k^{i,B} \sim \mathcal{N}(0, \sigma_m^2)$. Γ_k^i is a random non-negative delay with a sight-dependent probability distribution, i.e., $\Gamma_k^i | z_k^i \sim F_{z_k^i}$ (see Section 2.3). Let us note that the expression between parentheses in the first term corresponds to the actual receiving time.
4. The mobile sends a message back to the anchor after a short time δ. This message contains the reception time τ_k^i as measured by the mobile node. As it was explained in Section 1, δ is set large enough so that it can accommodate any reply processing delays in the mobile node. The actual

reply time is

$$t_k^{i,C} = t_k + i\Delta + n_k^{i,A} + \frac{d_k^i}{c} + \Gamma_k^i + \frac{\delta}{\omega_k} + \frac{n_k^{i,B} + n_k^{i,C}}{\omega_k}, \qquad (18)$$

where $n_k^{i,C} \sim \mathcal{N}(0, \sigma_m^2)$ and the presence of ω_k in the denominator of the last two terms is due to the fact that, because of its local clock inaccuracies, the mobile node fails to comply with the specified reply delay time δ.

5. The reference node receives this last message at a measured time

$$\tau_k^{i,D} = t_k^{i,C} + \frac{d_k^i}{c} + \Gamma_k^i + n_k^{i,D}, \qquad (19)$$

where $n_k^{i,D} \sim \mathcal{N}(0, \sigma_m^2)$. Observe that we assume that the mobile position and the sight condition do not vary significantly during a message exchange. Both assumptions are reasonable if δ is kept small.

As a result of this message exchange, only the values of τ_k^i and $\mathrm{T}_k^i = (\tau_k^{i,D} - t_k - \Delta i - \delta)/2$ for each anchor node are kept as observations. Let us note that

$$\mathrm{T}_k^i = \frac{d_k^i}{c} + \Gamma_k^i + \frac{\delta}{2}\left(\frac{1}{\omega_k} - 1\right) + n_k^{i,A} + n_k^{i,D} + \frac{n_k^{i,B} + n_k^{i,C}}{\omega_k}. \qquad (20)$$

Since this expression does not include ϕ_k, the values T_k^i are insufficient to track the clock at the mobile node and, thence, the need to record the values τ_k^i. In the presence of a perfect clock and noiseless time measurements, Eq. 20 reduces to

$$c \times \mathrm{T}_k^i = d_k^i + c \times \Gamma_k^i, \qquad (21)$$

which is exactly the same as Eq. (6) in the Introduction.

It is instructive to rewrite the observations assuming noiseless measurements in a LOS scenario. In this case, we have

$$\tau_k^i = \omega_k \times \left(t_k + i\Delta + \frac{d_k^i}{c}\right) + \phi_k, \qquad (22)$$

$$\mathrm{T}_k^i = \frac{d_k^i}{c} + \frac{\delta}{2}\left(\frac{1}{\omega_k} - 1\right). \qquad (23)$$

Since the state vector $\vec{s}_k$ has six components and there are $2 \times N_a$ observations, at least three anchor nodes are needed to estimate the system state. If more other sight conditions are considered, more information is needed and we turn to that problem in following section.

3.2. Sight Condition Statistic

As it was explained in the Introduction, we avoid any details of the underlying physical channel by assuming that any information on the sight condition, which can be inferred from the wireless signal, is summarized in a test statistic. Thus, to the observations τ_k^i and T_k^i, we add the values of the statistics ζ_k^i, $i = 0, 1, \cdots, N_a$, which provide an indication of the type of sight condition present during the message exchange between the mobile node and the ith reference node.

We assume that the distribution of the test statistic conditional on each sight situation is known. This distribution can be estimated from the definition of the statistic and previous knowledge about the sight condition based on a prior onsite survey. For the sake of clarity, let us call $p(\zeta | z = i)$ the probability density function of the test statistic ζ given that the sight situation is $z = i$.

3.3. Summary of the Observation Model

Observations at each measurement round can be summarized by the vectors

$$\vec{y}_k = \left(\tau_k^0,\, \mathrm{T}_k^0,\, \cdots,\, \tau_k^{N_a - 1},\, \mathrm{T}_k^{N_a - 1} \right)^T, \tag{24}$$

$$\vec{\zeta}_k = \left(\zeta_k^0,\, \cdots,\, \zeta_k^{N_a - 1} \right)^T, \tag{25}$$

where the conditional distributions of $\vec{y}_k$ and $\vec{\zeta}_k$ given $\vec{s}_k$ and $\vec{z}_k$ are known. Under this setting, our problem is to estimate the system state $\vec{s}_k$ based on $\vec{y}_k$ and $\vec{\zeta}_k$, where $\vec{z}_k$ can be considered a vector of nuisance parameters.

From Eqs. (17) and (20), it is clear that we can write

$$\vec{y}_k = \vec{h}(\vec{s}_k, \vec{\Gamma}_k, \vec{n}_k^{'}), \tag{26}$$

where $\vec{h}$ is a nonlinear function, and

$$\vec{\Gamma}_k = \left(\Gamma_k^0, \cdots, \Gamma_k^{N_a-1}\right)^T, \tag{27}$$

$$\vec{n}_k^{'} = \left(n_k^{0,A}, n_k^{0,B}, n_k^{0,C}, n_k^{0,D}, \cdots, n_k^{N_a-1,D}\right)^T. \tag{28}$$

The noise vector $\vec{n}_k^{'} \in \mathbb{R}^{4(N_a-1)}$ has a Gaussian distribution. Given the sight conditions $\vec{z}_k$, the distribution of $\vec{\Gamma}_k \in \mathbb{R}^{N_a-1}$ is known, but it may be, in general, non-Gaussian. For reasons that will become apparent in the next section, it is convenient to write the observation function as depending only on normally distributed random variables. This is indeed possible because it can be shown that a random variable with any arbitrary distribution can be expressed as the (possibly nonlinear) transformation of another variable with a Gaussian distribution. Therefore, given $\vec{z}_k$ we may write, with some abuse of notation,

$$\vec{y}_k = \vec{h}(\vec{s}_k, \vec{n}_k | \vec{z}_k), \tag{29}$$

where $\vec{n}_k \sim \mathcal{N}(\vec{0}, \mathbf{R}^n)$, $\mathbf{R}^n = \sigma_m^2 \mathbf{I}$ with $\mathbf{I}$ the identity matrix in $\mathbb{R}^{5(N_a-1)\times 5(N_a-1)}$.

4. Estimation Algorithm

Since observations τ_k^i and T_k^i depend nonlinearly on the mobile position and velocity, we can use an algorithm such as the Unscented Kalman Filter (UKF) [79–82] to track the state vector $\vec{s}_k$. The Unscented Kalman Filter, which is briefly outlined in Algorithm 1 for the sake of reference, approximates the posterior distribution of the parameters given the observations by a Gaussian density represented by a few selected deterministic samples known as sigma points. These sample points allow to compute the true mean and covariance up to a second order of the Taylor expansion of any nonlinear function.

If we want to apply UKF to our problem, we have to start with the definition of the functions $\vec{f}$ and $\vec{h}$ in Eq. (30) (see Algorithm 1). Function $\vec{f}$ describes the evolution of the state vector $\vec{s}_k$ and it is explicitly written for our case in Eq. (14). However, we cannot find the observation function $\vec{h}$. The closest description is

Algorithm 1: Unscented Kalman Filter

Model: The state vector $\vec{s}_k$ and the observation vector $\vec{y}_k$ are modeled by

$$\vec{s}_k = \vec{f}\left(\vec{s}_{k-1}, \vec{u}_{k-1}\right), \qquad \vec{y}_k = \vec{h}\left(\vec{s}_k, \vec{n}_k\right), \tag{30}$$

where $\vec{f}(\cdot)$ and $\vec{h}(\cdot)$ are two nonlinear functions, $\vec{u}_{k-1} \sim \mathcal{N}(0, \mathbf{R}^u)$ is a vector of innovations and $\vec{n}_k \sim \mathcal{N}(0, \mathbf{R}^n)$ is a noise vector.

Computation of sigma points:

$$\mathcal{S}^0_{k-1} = \hat{s}_{k-1},\ \mathcal{S}^l_{k-1} = \hat{s}_{k-1} + \gamma\left(\sqrt{\mathbf{P}^S_{k-1}}\right)_l,\ \mathcal{S}^{l+L}_{k-1} = \hat{s}_{k-1} - \gamma\left(\sqrt{\mathbf{P}^S_{k-1}}\right)_l,$$

for $l = 1, \cdots, L$, where $\mathbf{P}^S_{k-1} = \text{block-diag}(\mathbf{P}_{k-1}, \mathbf{R}^u, \mathbf{R}^n)$ and the sub-index l indicates the lth column.

Time update:

$$\mathcal{S}^{s,l}_{k|k-1} = \vec{f}(\mathcal{S}^{s,l}_{k-1}, \mathcal{S}^{u,l}_{k-1}), \qquad \hat{s}_{k|k-1} = \sum_{l=0}^{2L} W^{(m)}_l \mathcal{S}^{s,l}_{k|k-1}, \tag{31}$$

$$\mathcal{Y}^l_{k|k-1} = \vec{h}(\mathcal{S}^{s,l}_{k|k-1}, \mathcal{S}^{n,l}_{k|k-1}), \qquad \hat{y}_{k|k-1} = \sum_{l=0}^{2L} W^{(m)}_l \mathcal{Y}^l_{k|k-1}, \tag{32}$$

$$\mathbf{P}_{ss} = \sum_{l=0}^{2L} W^{(c)}_l \left[\mathcal{S}^{s,l}_{k|k-1} - \hat{s}_{k|k-1}\right]\left[\mathcal{S}^{s,l}_{k|k-1} - \hat{s}_{k|k-1}\right]^T, \tag{33}$$

$$\mathbf{P}_{yy} = \sum_{l=0}^{2L} W^{(c)}_l \left[\mathcal{Y}^l_{k|k-1} - \hat{y}_{k|k-1}\right]\left[\mathcal{Y}^l_{k|k-1} - \hat{y}_{k|k-1}\right]^T, \tag{34}$$

$$\mathbf{P}_{sy} = \sum_{l=0}^{2L} W^{(c)}_l \left[\mathcal{S}^{s,l}_{k|k-1} - \hat{s}_{k|k-1}\right]\left[\mathcal{Y}^l_{k|k-1} - \hat{y}_{k|k-1}\right]^T, \tag{35}$$

where the supra-indices s, u and n denote the rows corresponding to the state, the innovations and the noise, respectively.

Measurement update:

$$\mathcal{K} = \mathbf{P}_{sy}\mathbf{P}^{-1}_{yy},\ \hat{s}_k = \hat{s}_{k|k-1} + \mathcal{K}\cdot(\vec{y}_k - \hat{y}_{k|k-1}),\ \mathbf{P}_k = \mathbf{P}_{ss} - \mathcal{K}\cdot\mathbf{P}_{yy}\cdot\mathcal{K}^T.$$

For the values of γ, $W^{(m)}_l$ and $W^{(c)}_l$ see Ref. [79].

that in Eq. (29), where it is expressed conditional on the knowledge of the vector of sight situations $\vec{z}_k$. Therefore, UKF cannot be straightforwardly applied, as in our case we have to deal with varying statistical conditions depending on the unknown sight situations. Huerta et al. [51] proposed a modification of the UKF, the so-called Improved Unscented Kalman Filter (IUKF), to deal precisely with this problem. The IUKF uses several sets of sigma points, one for each possible sight situation, and estimates the system state $\vec{s}_k$ by weighting the results from each set. The weights are the posterior probabilities of each sight condition based on the known transition probabilities and the sight test statistics. In particular, let us call $\hat{P}(z_{k-1}^i = j)$ the estimated probability that $z_{k-1}^i = j$. Then, the posterior probability given the test statistic ζ_k^i can be estimated by

$$\hat{P}(z_k^i = j) \propto p(\zeta_k^i | z_k^i = j) \sum_{m=0}^{N_z-1} P(z_k^i = j | z_{k-1}^i = m) \hat{P}(z_{k-1}^i = m), \qquad (36)$$

where $P(z_k^i = j | z_{k-1}^i = m)$ is the known transition probability from sight condition m to sight condition j at time t_k (see Eq. (16)) and $p(\zeta_k^i | z_k^i = j)$ is the probability density function of the test statistic given the sight condition.

Note that the predicted observations in Eq. (32) (see Algorithm 1) depend on the assumed values of the sight condition for each mobile-anchor channel. IUKF proceeds by re-writing Eq. (32) as

$$\mathcal{Y}_{k|k-1}^{i,l} = \sum_{j=0}^{N_z-1} \hat{P}(z_k^i = j) \vec{h}^i \left(\mathcal{S}_{k|k-1}^{s,l}, \mathcal{S}_{k|k-1}^{n,l} \middle| z_k^i = j \right), \qquad (37)$$

where the supra-index i indicates the rows corresponding to the ith reference node and $\vec{h}^i(\cdot | z_k^i = j)$ is the observation function given the sight condition $z_k^i = j$ (cf. Eq. (29)). The remaining steps of IUKF are as in UKF.

Since IUKF needs an initial state guess, we find a rough estimate by considering only two message exchanges and assuming LOS in all paths, as it was done in Ref. [17]. The reader is referred to that work for more details.

It must be emphasized that our approach is very different to that in Huerta et

Table 1: Main simulation parameters

σ_ω	10^{-11}	σ_ϕ	10^{-2} ns	σ_v	$0.1\ \mathrm{m\,s^{-1}}$
ω_0	$1 - 10^{-5}$	ϕ_0	500 ns	σ_m	0.2 ns
h	1 ms	Δ	5 µs	δ	1 µs

σ_ω, σ_ϕ and σ_v are the standard deviations of the steps in the Gaussian random walks modeling the evolution of the clock skew ω, the clock offset ϕ and each component of the mobile velocity $\vec{v}$, respectively. Initial skew and offset are denoted by ω_0 and ϕ_0, respectively. σ_m is the standard deviation of the time measurement noise.
h is the time between measurement rounds, Δ is the time between message exchanges, and δ is the nominal reply delay by the mobile (see Fig. 1).

al. [51], although we adapt the Improved Unscented Kalman Filter to our problem and we make use of a test statistic that indicates the presence of NLOS. Indeed, Ref. [51] deals with only two sight conditions (LOS and NLOS), it does not consider clock inaccuracies, and uses a much simpler time measurement scheme. For the sake of reference, we shall call our algorithm Time-Synchronization IUKF (TS-IUKF).

5. Numerical Experiments

In this section we present numerical results corresponding to different scenarios. First, we consider examples with three sight conditions, one LOS and two different NLOS situations. Then we turn to simpler examples that enable us to compare the performance of our proposal to that of other well-known algorithms in the literature. In order to conduct a fairer comparison, we use simpler scenarios with only two sight conditions, LOS and one NLOS, and either a perfect clock or a stationary node.

5.1. Three Sight Conditions

Table 1 presents the main simulation parameters. Although our proposed algorithm can be extended to more complex scenarios, we assume three possible sight situations, LOS, hard NLOS and soft NLOS (see Section 1). We adapt the four-state model in Ref. [44] and fix the transition probability matrix to

$$\mathbf{Q} = \begin{pmatrix} 0.970 & 0.010 & 0.020 \\ 0.010 & 0.970 & 0.020 \\ 0.025 & 0.025 & 0.950 \end{pmatrix}, \tag{38}$$

where the states are in the following order: LOS, hard NLOS, soft NLOS. We model changes in the state of this Markov chain as occurring only at integer K_{sight} multiples of the observation interval h. In particular, we use $K_{\text{sight}} = 1000$ and 150 when the initial mean mobile speed is zero and 1 $\mathrm{m\,s^{-1}}$, respectively. Intuitively, the sight condition is expected to change more frequently as the mobile moves faster.

Following Ref. [44], we model Γ as a normal random variable with mean μ_{sNLOS} and variance σ^2_{sNLOS} in the soft NLOS situation, and with a generalized extreme value distribution $\text{GEV}(k_{\text{hNLOS}}, \mu_{\text{hNLOS}}, \sigma^2_{\text{hNLOS}})$ in the hard NLOS case. The parameters used for simulations are $\mu_{\text{sNLOS}} = 0.35$ ns, $\sigma_{\text{sNLOS}} = 0.07$ ns, $\mu_{\text{hNLOS}} = 8.5$ ns, $\sigma_{\text{hNLOS}} = 4.25$ ns, $k_{\text{hNLOS}} = 0.4$. In the LOS situation, we simply assume $\Gamma = 0$.

The probability densities of the test statistic given each sight condition are shown in Fig. 2. These distributions have been chosen so it is difficult to distinguish LOS and soft NLOS conditions. Besides this fact, they are arbitrary and solely for the purpose of simulations.

Reference nodes are uniformly and deterministically distributed on a circumference with a 100 m radius. At the beginning of each simulation, the mobile node is located at the center of that circumference.

Figures 3-4 show results for TS-IUKF when considering all clock inaccuracies (skew and offset) and three line-of-sight conditions, for five reference nodes ($N_a = 5$). The accuracy in the estimation of the state parameters in $\vec{s}_k$ is measured as the root-mean-square error resulting from an average of 250 realizations. We also include the Cramér-Rao bound found in Ref. [17] for the LOS-only case. As it can be observed, not only the performance of our proposed algorithm improves over time, but it also reaches a positioning accuracy in the order of centimeters. We also explore the effect of varying the number of anchors in Fig. 5. As expected, the localization error improves as more reference nodes are added and an order of magnitude improvement is obtained when going from $N_a = 3$ to $N_a = 15$. All in all, we find that our proposed solution effectively tracks the mobile node and its clock.

5.2. Two Sight Conditions

It is interesting to compare the performance of our proposed algorithm to that of two well-established approaches such as Rwgh [22] and QP [26]. Since these algorithms consider only two sight conditions and in order to make a fairer comparison, we adapt our modeling setup in the previous section to a simpler LOS/hard-NLOS scenario, with a transition probability matrix is given by

$$\mathbf{Q} = \begin{pmatrix} 0.970 & 0.030 \\ 0.030 & 0.970 \end{pmatrix}. \tag{39}$$

It must be noted that these algorithms use only the estimated distances between the mobile node and each anchor node. In terms of the measurements in our

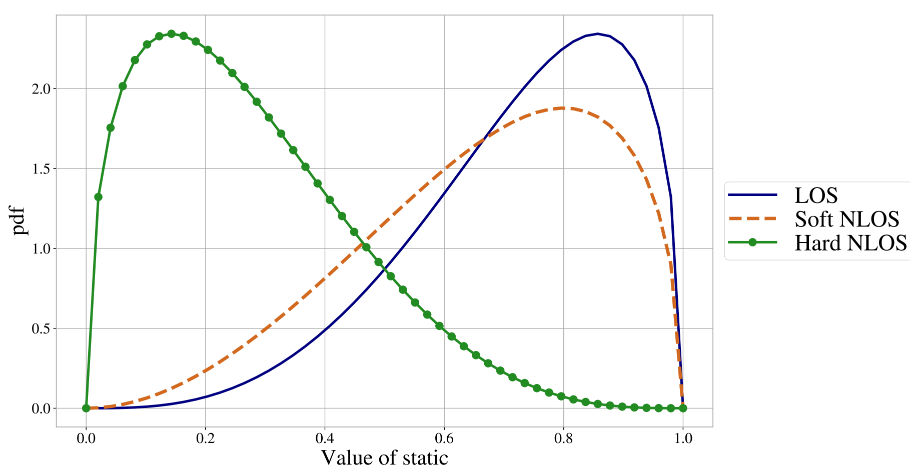

Figure 2: Probability density of the test statistic conditional on the sight condition: Beta(4.0, 1.5) in the case of LOS (solid blue), Beta(3.0, 1.5) in the case of soft NLOS (dotted green), and Beta(1.5, 4.0) for hard NLOS (dashed orange).

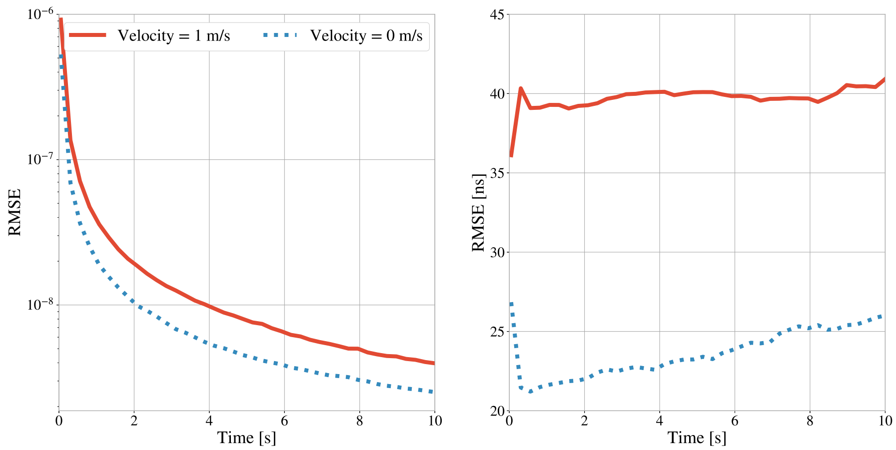

Figure 3: RMSE of the TS-IUKF algorithm for the skew (left) and the offset (right), when the mean mobile speed is 0 $\mathrm{m\,s^{-1}}$ (blue dotted line) and 1 $\mathrm{m\,s^{-1}}$ (solid red line). Three line-of-sight conditions and all clock inaccuracies are considered.

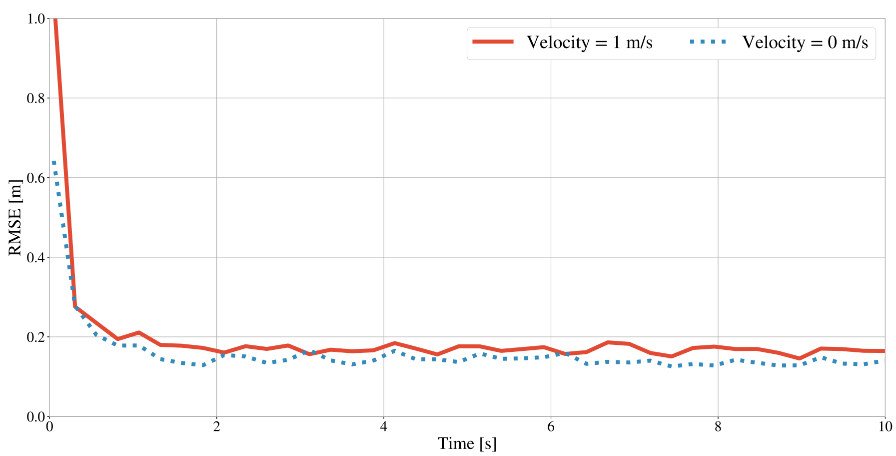

Figure 4: RMSE of the TS-IUKF algorithm for the position when the mean mobile speed is 0 $\mathrm{m\,s^{-1}}$ (blue dotted line) and 1 $\mathrm{m\,s^{-1}}$ (solid red line). Three line-of-sight conditions and all clock inaccuracies are considered.

protocol, we assume that estimated distances correspond to $c \cdot \mathrm{T}_k^i$. Furthermore, Rwgh and QP do not take into account clock inaccuracies. For this reason, we present results for a stationary mobile node ($\sigma_v = 0\ \mathrm{m\,s^{-1}}$) with a perfect clock and $N_a = 5$ in Fig. 6. As it can be observed, TS-IUKF is the best performing algorithm.Figure 7 shows results for a mobile node with a mean speed of 1 $\mathrm{m\,s^{-1}}$.

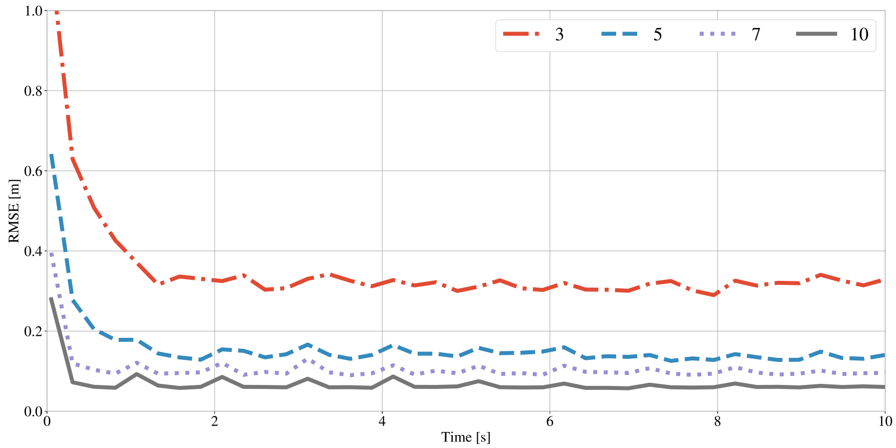

Figure 5: RMSE of the TS-IUKF algorithm for the position of the mobile node when using different numbers of reference nodes. Improvement is appreciated as the number of anchors increases. Three line-of-sight conditions and all clock inaccuracies are considered, and the mean velocity is 0 $\mathrm{m\,s^{-1}}$.

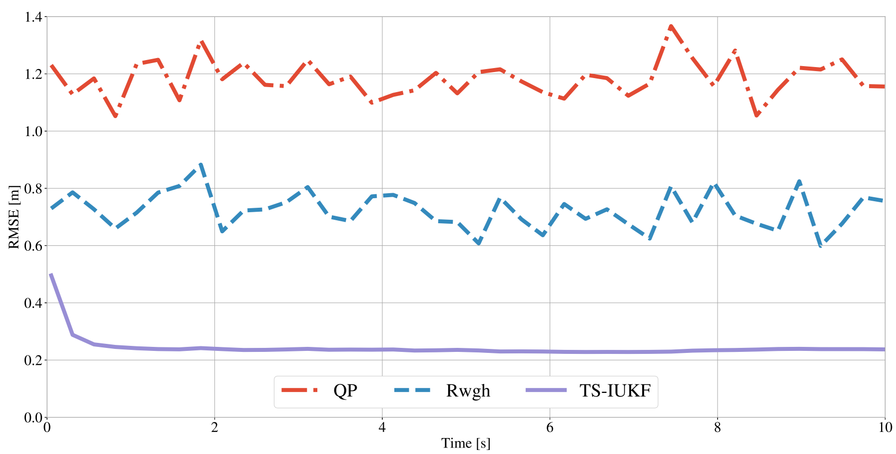

Figure 6: Position RMSE of QP (dash-dotted red line), Rwgh (dashed blue line), and TS-IUKF (solid violet line). TS-IUKF outperforms the other algorithms. Two line-of-sight conditions and a perfect clock at a stationary mobile are considered.

As it can be observed, while TS-IUKF performs similarly as in the stationary node case,the performance of Rwgh and QP is much worse.

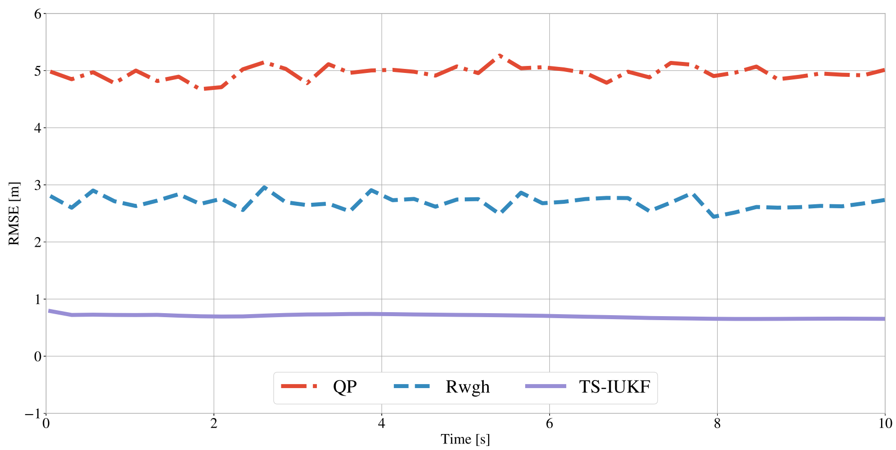

Figure 7: Position RMSE of QP (dash-dotted red line), Rwgh (dashed blue line), and TS-IUKF (solid violet line). TS-IUKF outperforms the other algorithms. Two line-of-sight conditions and a perfect clock at node moving with a 1 $\mathrm{m\,s^{-1}}$ speed are considered.

6. Conclusion

We have presented an approach to simultaneously track the position and velocity of a wireless node, and the skew and offset of its clock, under varying sight conditions of the links between the node and a set of anchors. To the best of our knowledge, this is the first proposal to tackle this problem.

We have shown, by means of simulations, that our proposal (TS-IUKF) yields good results. Furthermore, we have compared its performance to that of other well-established localization algorithms in the literature, showing that TS-IUKF has lower localization errors.

One of the shortcomings of our proposal is the need for an offline site survey to estimate the distributions of the NLOS delays and the transition probability matrix of the Markov chain. A possible alternative for the estimation of the transition probabilities might be the use of a technique such as the Baum-Welch algorithm [83]. Indeed, changes in the sight condition can be represented as a hidden-Markov model where the corresponding observations are the test statistics ζ_k^i. The investigation of this and other alternatives is a matter of future work which is needed in order to facilitate the real-world implementation of the algorithm.

Acknowledgment

This work was funded by the project PID 2015 # 3 from the Agencia Nacional de Promoción de la Investigación, el Desarrollo Tecnológico y la Innovación (ANPCyT), Argentina.

References

[1] Z. Sahinoglu, S. Gezici, I. Guvenc, Ultra-wideband Positioning Systems, Cambridge, 2008.

[2] J. Figueiras, S. Frattasi, Mobile Positioning and Tracking: From Conventional to Cooperative Techniques, John Wiley & Sons, 2010.

[3] J. Cheng, L. Yang, Y. Li, W. Zhang, Seamless outdoor/indoor navigation with WIFI/GPS aided low cost inertial navigation system, Physical Communication 13 (2014) 31–43.

[4] A. Bensky, Wireless Positioning Technologies and Applications, Artech House, 2016.

[5] F. Zafari, A. Gkelias, K. K. Leung, A survey of indoor localization systems and technologies, IEEE Communications Surveys and Tutorials 21 (3) (2019) 2568–2599.

[6] H. Gu, K. Zhao, C. Yu, Z. Zheng, High resolution time of arrival estimation algorithm for B5G indoor positioning, Physical Communication 50 (2022) 101494.

[7] A. Kumar, P. A. Koch, H. E. Baidoo-Williams, R. Mudumbai, S. Dasgupta, An empirical study of the statistics of phase drift of off-the-shelf oscillators for distributed MIMO applications, in: 2014 IEEE International Symposium on Dynamic Spectrum Access Networks (DYSPAN), IEEE, 2014, pp. 350–353.

[8] J. McNeill, S. Razavi, K. Vedula, D. R. Brown, Experimental characterization and modeling of low-cost oscillators for improved carrier phase synchronization, in: 2017 IEEE International Instrumentation and Measurement Technology Conference (I2MTC), IEEE, 2017, pp. 1–6.

[9] F. Tirado-Andrés, A. Araujo, Performance of clock sources and their influence on time synchronization in wireless sensor networks, International Journal of Distributed Sensor Networks 15 (9) (2019) 1550147719879372.

[10] H. Kim, X. Ma, B. R. Hamilton, Tracking low-precision clocks with time-varying drifts using Kalman filtering, IEEE/ACM Transactions on Networking 20 (1) (2012) 257–270.

[11] M. Koivisto, M. Costa, J. Werner, K. Heiska, J. Talvitie, K. Leppanen, V. Koivunen, M. Valkama, Joint device positioning and clock synchronization in 5G ultra-dense networks, IEEE Transactions on Wireless Communications 16 (5) (2017) 2866–2881.

[12] A. Mahmood, R. Exel, H. Trsek, T. Sauter, Clock synchronization over IEEE 802.11 - A survey of methodologies and protocols, IEEE Transactions on Industrial Informatics 13 (2) (2017) 907–922.

[13] Y.-C. Wu, Q. Chaudhari, E. Serpedin, Clock synchronization of wireless sensor networks, IEEE Signal Processing Magazine 28 (1) (2010) 124–138.

[14] N. M. Freris, S. R. Graham, P. Kumar, Fundamental limits on synchronizing clocks over networks, IEEE Transactions on Automatic Control 56 (6) (2010) 1352–1364.

[15] B. Etzlinger, H. Wymeersch, A. Springer, Cooperative synchronization in wireless networks, IEEE Transactions on Signal Processing 62 (11) (2014) 2837–2849.

[16] X. Huan, K. S. Kim, On the practical implementation of propagation delay and clock skew compensated high-precision time synchronization schemes

with resource-constrained sensor nodes in multi-hop wireless sensor networks, Computer Networks 166 (2020) 106959.

[17] J. P. Grisales Campeón, P. I. Fierens, Joint position and clock tracking of wireless nodes, Computer Networks 197 (2021) 108296.

[18] B. Denis, J. B. Pierrot, C. Abou-Rjeily, Joint distributed synchronization and positioning in UWB Ad Hoc networks using TOA, IEEE Transactions on Microwave Theory and Techniques 54 (4) (2006) 1896–1910.

[19] J. Zheng, Y.-C. Wu, Joint Time Synchronization and Localization of an Unknown Node in Wireless Sensor Networks, IEEE Transactions on Signal Processing 58 (3) (2009) 1309–1320.

[20] S. P. Chepuri, R. T. Rajan, G. Leus, A.-J. Van der Veen, Joint clock synchronization and ranging: Asymmetrical time-stamping and passive listening, IEEE Signal Processing Letters 20 (1) (2012) 51–54.

[21] S. Wu, S. Zhang, D. Huang, A TOA-based localization algorithm with simultaneous NLOS mitigation and synchronization error elimination, IEEE Sensors Letters 3 (3) (2019) 1–4.

[22] P.-C. Chen, A non-line-of-sight error mitigation algorithm in location estimation, in: WCNC. 1999 IEEE Wireless Communications and Networking Conference (Cat. No.99TH8466), Vol. 1, 1999, pp. 316–320 vol.1.

[23] L. Cong, W. Zhuang, Non-line-of-sight error mitigation in TDOA mobile location, in: GLOBECOM'01. IEEE Global Telecommunications Conference (Cat. No. 01CH37270), Vol. 1, IEEE, 2001, pp. 680–684.

[24] S. Al-Jazzar, J. Caffery, H.-R. You, A scattering model based approach to NLOS mitigation in TOA location systems, in: IEEE 55th Vehicular Technology Conference. VTC Spring 2002 (Cat. No. 02CH37367), Vol. 2, IEEE, 2002, pp. 861–865.

[25] S. Al-Jazzar, J. Caffery, ML and Bayesian TOA location estimators for NLOS environments, in: Proceedings IEEE 56th Vehicular Technology Conference, Vol. 2, IEEE, 2002, pp. 1178–1181.

[26] X. Wang, Z. Wang, B. O'Dea, A TOA-based location algorithm reducing the errors due to non-line-of-sight (NLOS) propagation, IEEE Transactions on Vehicular Technology 52 (1) (2003) 112–116.

[27] B. L. Le, K. Ahmed, H. Tsuji, Mobile location estimator with NLOS mitigation using Kalman filtering, in: IEEE Wireless Communications and Networking, 2003. WCNC 2003., Vol. 3, IEEE, 2003, pp. 1969–1973.

[28] B. Denis, J. Keignart, N. Daniele, Impact of NLOS propagation upon ranging precision in UWB systems, in: IEEE conference on Ultra Wideband Systems and Technologies, 2003, IEEE, 2003, pp. 379–383.

[29] S. Gezici, H. Kobayashi, H. V. Poor, Nonparametric nonline-of-sight identification, in: IEEE 58th Vehicular Technology Conference. VTC 2003-Fall (IEEE Cat. No. 03CH37484), Vol. 4, IEEE, 2003, pp. 2544–2548.

[30] M. Najar, J. Vidal, Kalman tracking for mobile location in NLOS situations, in: 14th IEEE Proceedings on Personal, Indoor and Mobile Radio Communications, 2003. PIMRC 2003., Vol. 3, IEEE, 2003, pp. 2203–2207.

[31] S. Venkatraman, J. Caffery, H.-R. You, A novel TOA location algorithm using LOS range estimation for NLOS environments, IEEE Transactions on Vehicular Technology 53 (5) (2004) 1515–1524.

[32] L. Cong, W. Zhuang, Nonline-of-sight error mitigation in mobile location, IEEE Transactions on Wireless Communications 4 (2) (2005) 560–573.

[33] J.-F. Liao, B.-S. Chen, Robust mobile location estimator with NLOS mitigation using interacting multiple model algorithm, IEEE Transactions on Wireless Communications 5 (11) (2006) 3002–3006.

[34] J. M. Huerta, J. Vidal, LOS-NLOS Situation Tracking for Positioning Systems, in: 2006 IEEE 7th Workshop on Signal Processing Advances in Wireless Communications, 2006, pp. 1–5.

[35] Y. T. Chan, W. Y. Tsui, H. C. So, P. C. Ching, Time-of-arrival based localization under NLOS conditions, IEEE Transactions on Vehicular Technology 55 (1) (2006) 17–24.

[36] K. Pahlavan, F. O. Akgul, M. Heidari, A. Hatami, J. M. Elwell, R. D. Tingley, Indoor geolocation in the absence of direct path, IEEE Wireless Communications 13 (6) (2006) 50–58.

[37] S. Venkatesh, R. M. Buehrer, A linear programming approach to NLOS error mitigation in sensor networks, Proceedings of the Fifth International Conference on Information Processing in Sensor Networks, IPSN '06 2006 (2006) 301–308.

[38] F. Li, W. Xie, J. Wang, S. Liu, A new two-step ranging algorithm in NLOS environment for UWB systems, in: 2006 Asia-Pacific Conference on Communications, IEEE, 2006, pp. 1–5.

[39] C. Ma, R. Klukas, G. Lachapelle, A nonline-of-sight error-mitigation method for TOA measurements, IEEE Transactions on Vehicular Technology 56 (2) (2007) 641–651.

[40] S. Al-Jazzar, J. Caffery, H.-R. You, Scattering-model-based methods for TOA location in NLOS environments, IEEE Transactions on Vehicular Technology 56 (2) (2007) 583–593.

[41] İ. Güvenç, C.-C. Chong, F. Watanabe, NLOS identification and mitigation for UWB localization systems, in: 2007 IEEE Wireless Communications and Networking Conference, IEEE, 2007, pp. 1571–1576.

[42] İ. Güvenç, C.-C. Chong, F. Watanabe, H. Inamura, NLOS identification and weighted least-squares localization for UWB systems using multipath

channel statistics, EURASIP Journal on Advances in Signal Processing 2008 (1) (2007) 271984.

[43] H. Miao, K. Yu, M. J. Juntti, Positioning for NLOS propagation: Algorithm derivations and Cramer–Rao bounds, IEEE Transactions on Vehicular Technology 56 (5) (2007) 2568–2580.

[44] M. Heidari, K. Pahlavan, A Markov model for dynamic behavior of ranging errors in indoor geolocation systems, IEEE Communications Letters 11 (12) (2007) 934–936.

[45] M. Heidari, K. Pahlavan, A Markov model for dynamic behavior of ToA-based ranging in indoor localization, EURASIP Journal on Advances in Signal Processing 2008 (2007) 1–14.

[46] S. Mazuelas, F. A. Lago, J. Blas, A. Bahillo, P. Fernandez, R. M. Lorenzo, E. J. Abril, Prior NLOS measurement correction for positioning in cellular wireless networks, IEEE Transactions on Vehicular Technology 58 (5) (2008) 2585–2591.

[47] S. Al-Jazzar, M. Ghogho, D. McLernon, A joint TOA/AOA constrained minimization method for locating wireless devices in non-line-of-sight environment, IEEE Transactions on Vehicular Technology 58 (1) (2009) 468–472.

[48] Y. Xie, Y. Wang, P. Zhu, X. You, Grid-search-based hybrid TOA/AOA location techniques for NLOS environments, IEEE Communications Letters 13 (4) (2009) 254–256.

[49] A. Abbasi, M. H. Kahaei, Improving source localization in LOS and NLOS multipath environments for UWB signals, in: 2009 14th International CSI Computer Conference, IEEE, 2009, pp. 310–316.

[50] L. Chen, L. Wu, Mobile positioning in mixed LOS/NLOS conditions using modified EKF banks and data fusion method, IEICE Transactions on Communications 92 (4) (2009) 1318–1325.

[51] J. M. Huerta, J. Vidal, A. Giremus, J. Y. Tourneret, Joint Particle Filter and UKF Position Tracking in Severe Non-Line-of-Sight Situations, IEEE Journal on Selected Topics in Signal Processing 3 (5) (2009) 874–888.

[52] D. Dardari, A. Conti, U. Ferner, A. Giorgetti, M. Z. Win, Ranging with ultrawide bandwidth signals in multipath environments, Proceedings of the IEEE 97 (2) (2009) 404–426.

[53] I. Guvenc, C.-C. Chong, A Survey on TOA Based Wireless Localization and NLOS Mitigation Techniques, IEEE Communications Surveys & Tutorials 11 (3) (2009) 107–124.

[54] J. Khodjaev, Y. Park, A. Saeed Malik, Survey of NLOS identification and error mitigation problems in UWB-based positioning algorithms for dense environments, Annals of Telecommunications-Annales des Télécommunications 65 (5) (2010) 301–311.

[55] S. Maranò, W. M. Gifford, H. Wymeersch, M. Z. Win, NLOS identification and mitigation for localization based on UWB experimental data, IEEE Journal on Selected Areas in Communications 28 (7) (2010) 1026–1035.

[56] M. Boccadoro, G. De Angelis, P. Valigi, TDOA positioning in NLOS scenarios by particle filtering, Wireless Networks 18 (5) (2012) 579–589.

[57] G. Wang, H. Chen, Y. Li, N. Ansari, NLOS error mitigation for TOA-based localization via convex relaxation, IEEE Transactions on Wireless Communications 13 (8) (2014) 4119–4131.

[58] D. Liu, K. Liu, Y. Ma, J. Yu, Joint toa and doa localization in indoor environment using virtual stations, IEEE Communications Letters 18 (8) (2014) 1423–1426.

[59] Z. Abu-Shaban, X. Zhou, T. D. Abhayapala, A novel TOA-based mobile localization technique under mixed LOS/NLOS conditions for cellular networks, IEEE Transactions on Vehicular Technology 65 (11) (2016) 8841–8853.

[60] J. M. Pak, C. K. Ahn, P. Shi, Y. S. Shmaliy, M. T. Lim, Distributed hybrid particle/FIR filtering for mitigating NLOS effects in TOA-based localization using wireless sensor networks, IEEE Transactions on Industrial Electronics 64 (6) (2016) 5182–5191.

[61] Z. Su, G. Shao, H. Liu, Semidefinite programming for NLOS error mitigation in TDOA localization, IEEE Communications Letters 22 (7) (2017) 1430–1433.

[62] K. Gururaj, A. K. Rajendra, Y. Song, C. L. Law, G. Cai, Real-time identification of NLOS range measurements for enhanced UWB localization, in: 2017 International Conference on Indoor Positioning and Indoor Navigation (IPIN), IEEE, 2017, pp. 1–7.

[63] R. Mendrzik, H. Wymeersch, G. Bauch, Z. Abu-Shaban, Harnessing NLOS components for position and orientation estimation in 5G millimeter wave MIMO, IEEE Transactions on Wireless Communications 18 (1) (2018) 93–107.

[64] K. Yu, K. Wen, Y. Li, S. Zhang, K. Zhang, A novel NLOS mitigation algorithm for UWB localization in harsh indoor environments, IEEE Transactions on Vehicular Technology 68 (1) (2018) 686–699.

[65] H. Xiong, M. Peng, S. Gong, Z. Du, A novel hybrid RSS and TOA positioning algorithm for multi-objective cooperative wireless sensor networks, IEEE Sensors Journal 18 (22) (2018) 9343–9351.

[66] X. Yang, F. Zhao, T. Chen, NLOS identification for UWB localization based on import vector machine, AEU - International Journal of Electronics and Communications 87 (2018) 128–133.

[67] L. Cheng, Y. Li, Y. Wang, Y. Bi, L. Feng, M. Xue, A triple-filter NLOS localization algorithm based on fuzzy c-means for wireless sensor networks, Sensors 19 (5).

[68] F. Wen, H. Wymeersch, B. Peng, W. P. Tay, H. C. So, D. Yang, A survey on 5G massive MIMO localization, Digital Signal Processing 94 (2019) 21–28.

[69] C. H. Park, J. H. Chang, Modified MM algorithm and Bayesian expectation maximization-based robust localization under NLOS contaminated environments, IEEE Access 9 (2021) 4059–4071.

[70] B. Alavi, K. Pahlavan, Modeling of the TOA-based distance measurement error using UWB indoor radio measurements, IEEE communications letters 10 (4) (2006) 275–277.

[71] A. F. Molisch, Ultrawideband propagation channels-theory, measurement, and modeling, IEEE Transactions on Vehicular Technology 54 (5) (2005) 1528–1545.

[72] V. Barral, C. J. Escudero, J. A. García-Naya, NLOS Classification Based on RSS and Ranging Statistics Obtained from Low-Cost UWB Devices, in: 2019 27th European Signal Processing Conference (EUSIPCO), 2019, pp. 1–5.

[73] F. Sivrikaya, B. Yener, Time synchronization in sensor networks: A survey, IEEE Network 18 (4) (2004) 45–50.

[74] R. T. Rajan, A. J. Van der Veen, Joint Ranging and Synchronization for an Anchorless Network of Mobile Nodes, IEEE Transactions on Signal Processing 63 (8) (2015) 1925–1940.

[75] C. McElroy, D. Neirynck, M. McLaughlin, Comparison of wireless clock synchronization algorithms for indoor location systems, in: 2014 IEEE International Conference on Communications Workshops (ICC), 2014, pp. 157–162.

[76] R. David, D. R. Brown, Modeling and tracking phase and frequency offsets in low-precision clocks, in: 2015 IEEE Aerospace Conference, IEEE, 2015, pp. 1–7.

[77] C. Zucca, P. Tavella, The clock model and its relationship with the Allan and related variances, IEEE Transactions on Ultrasonics, Ferroelectrics, and Frequency Control 52 (2) (2005) 289–295.

[78] T. Camp, J. Boleng, V. Davies, A survey of mobility models for ad hoc network research, Wireless Communications and Mobile Computing 2 (5) (2002) 483–502.

[79] E. A. Wan, R. Van Der Merwe, The Unscented Kalman filter for Nonlinear Estimation, in: Proceedings of the IEEE 2000 Adaptive Systems for Signal Processing, Communications, and Control Symposium (Cat. No. 00EX373), 2000, pp. 153–158.

[80] S. J. Julier, J. K. Uhlmann, New extension of the Kalman filter to nonlinear systems, in: I. Kadar (Ed.), Signal Processing, Sensor Fusion, and Target Recognition VI, Vol. 3068, International Society for Optics and Photonics, SPIE, 1997, pp. 182 – 193.

[81] S. J. Julier, J. K. Uhlmann, Unscented filtering and nonlinear estimation, Proceedings of the IEEE 92 (3) (2004) 401–422.

[82] E. A. Wan, R. Van der Merwe, The Unscented Kalman Filter, John Wiley & Sons, 2002, Ch. 7, pp. 221–280.

[83] L. E. Baum, T. Petrie, G. Soules, N. Weiss, A maximization technique occurring in the statistical analysis of probabilistic functions of Markov chains, The Annals of Mathematical Statistics 41 (1) (1970) 164–171.